ISSN 1070-3284, Russian Journal of Coordination Chemistry, 2016, Vol. 42, No. 2, pp. 129–136. © Pleiades Publishing, Ltd., 2016.

Two Naphthoate-Based Lead(II) Complexes with Different Limited-Nuclear Motifs: Syntheses, Crystal Structures, and Fluorescent Properties[1]

P. X. Dai

College of Chemistry and Environmental Science, Shaanxi University of Technology, Hanzhong, Shaanxi, 723001 P.R. China
Shaanxi Province Key Laboratory of Catalytic Fundamental & Applications,
Shaanxi University of Technology, Hanzhong, Shaanxi, 723001 P.R. China
e-mail: dpx@iccas.ac.cn

Received April 21, 2015

Abstract—Two new naphthoate-based lead(II) complexes, $[Pb(NA)_2(2,2'\text{-Bipy})]$ (**I**) and $[Pb_2(NA)_4(4,4'\text{-Bipy})]$ (**II**) (NA^- = 1-naphthoate, 2,2'-Bipy = 2,2'-bipyridine, and 4,4'-Bipy = 4,4'-bipyridine) (CIF files CCDC nos. 664900 (**I**), 664899 (**II**)) have been hydrothermally synthesized by varying the N-heterocyclic coligands. Structural analyses reveal that the two complexes possess different limited-nuclear motifs, the former one owns mononuclear unit and the last complex exhibits centrosymmetric binuclear motif bridged by 4,4'-Bipy connector. The coordination numbers of Pb(II) metal centers in **I** and **II** are four and five, respectively. The NA^- anions in both complexes show the same binding modes, it is obvious that the bipyridyl coligands in the present mixed-ligands system are responsible for the dissociation or dimerization of mononuclear structural units and the binding numbers of the metal ion. In both complexes, the 6*s* lone pair of electrons of Pb^{2+} has a stereochemistry activity resulting the distribution of the Pb–O and Pb–N bonds in a hemisphere. Furthermore, both of the two compounds are linked to 2D network by intermolecular C–H···O hydrogen bonding and π···π stacking interactions, exhibiting strong fluorescent emissions resulting from the NA^--based intraligand charge transfer at room temperature, which can be hopefully used as fluorescent materials.

DOI: 10.1134/S1070328416020020

INTRODUCTION

Over the past decades, the controllable design and construction of metal complexes have been rapidly developed not only for their intriguing structural and topology [1, 2], but also due to the potential applications in selective catalyst [3, 4], molecular separation [5], and functional materials [6, 7]. In this field, Pb(II) complexes have attracted remarkable attention because of the large radius like lanthanide ions, diverse binding numbers from two to twelve, rich coordination geometry, and the possible occurrence of a stereochemically active lone pair of electrons [8–10]. For high coordination numbers (9–12), the lone pair is stereochemically inactive and the metal-ligand bonds are distributed evenly throughout the coordination sphere, resulting in a holodirected geometry [8]. And Pb(II) complexes with low binding number (2–5) adopt hemidirected coordination environment in which the ligands are distributed unevenly around the metal center, and the identifiable void present in the coordination sphere probably ascribe into the stereochemically active lone pair [9]. On the contrary, the stereochemical activity of the lone pair and the coordination geometry of Pb(II) complex with intermediate binding number (6~8), depends strongly on the nature of ligands [10]. Although many Pb(II) complexes have been documented [8–13], it is still difficult to construct Pb(II) complexes with the desirable structure and property. To further survey the influence of auxiliary co-ligands on the structures and properties of Pb(II) coordination complexes, 2,2'-bipyridine (2,2'-Bipy) and 4,4'-bipyridine (4,4'-Bipy) were selected as co-ligands to construct lead(II) complexes based on 1-naphthoic acid (HNA). We choose HNA as the core-ligand based on the following considerations: (a) deprotonated 1-naphthoate (NA^-) with a three-atom carboxylate attached on a bulky π-conjugate naphthyl skeleton is capable of binding with metal ion; (b) the rigid naphthalene rings can be involved into weak π···π stacking and C–H···π interactions [14–17].

In the present contribution, two NA^--based Pb(II) complexes, $[Pb(NA)_2(2,2'\text{-Bipy})]$ (**I**) and $[Pb_2(NA)_4(4,4'\text{-Bipy})]$ (**II**) were hydrothermally

[1] The article is published in the original.

obtained and structurally characterized. Despite these two complexes possess similar limited-nuclear structures, **I** owns mononuclear unit and **II** exhibits binuclear motif, both of which are linked to 2D network by intermolecular C–H···O hydrogen bonding and π···π stacking interactions. Furthermore, both compounds exhibit strong fluorescent emissions at room temperature, which primarily resulted from the intraligand electronic transfer of NA^- anion.

EXPERIMENTAL

Reagents and instruments. HNA was purchased from Acros and other analytical-grade starting materials were obtained commercially and used as received without further purification. Doubly deionized water was employed for the conventional synthesis. IR spectra were collected in a range of 4000–400 cm^{-1} region on a Nicolet IR-200 spectrometer with KBr pellets. Elemental analyses for C, H and N were determined on a Perkin-Elmer 2400C elemental analyzer. Their mogravimetric analysis (TGA) experiments were carried out on a Shimadzu simultaneous DTG-60A thermal analysis instrument with a heating rate of 10°C min^{-1} from room temperature to 800°C under a nitrogen atmosphere (flow rate 10 mL min^{-1}). Fluorescence spectra of the polycrystalline powder samples of **I** and **II** were performed on a Fluorolog-3 fluorescence spectrophotometer from Horiba Jobin Yvon at room temperature.

Synthesis of I. A mixture of HNA (68.9 mg, 0.4 mmol), 2,2'-Bipy (62.4 mg, 0.4 mmol), $PbAc_2 \cdot 3H_2O$ (76 mg, 0.2 mmol), NaOH (24.0 mg, 0.6 mmol), and doubly deionized water (12 mL) were sealed in a 23 mL stainless steel vessel and heated at 160°C for 96 h under autogenous pressure. After the mixture was cooled to room temperature at the rate of 5°C h^{-1}, pale-yellow block-shaped crystals suitable for single-crystal X-ray diffraction analysis were isolated directly, washed with ethanol, and dried in air. The yield was 15% based on HNA ligand.

For $C_{34}H_{22}N_2O_4Pb$

anal. calcd., %:	C, 54.46;	H, 3.14;	N, 3.97.
Found, %:	C, 54.43;	H, 3.18;	N, 3.93.

IR (ν, cm^{-1}): 3051 ν(C–H), 1594 $\nu_{as}(COO^-)$, 1545 $\nu_{as}(COO^-)$, 1470 $\nu_s(COO^-)$, 1430 $\nu_s(COO^-)$, 1356 $\nu_s(COO^-)$.

Synthesis of II. Colorless prism-shaped crystals of **II** suitable for single-crystal X-ray diffraction analysis were obtained by adopting the similar procedures to those of **I** only with 4,4'-Bipy instead of 2,2'-Bipy. The yield was 56% based on HNA ligand.

For $C_{27}H_{18}NO_4Pb$

anal. calcd., %:	C, 51.67;	H, 2.89;	N, 2.23.
Found, %:	C, 51.71;	H, 2.83;	N, 2.26.

IR (ν, cm^{-1}): 3051 ν(C–H), 1598 $\nu_{as}(COO^-)$, 1541 $\nu_{as}(COO^-)$, 1456 $\nu_s(COO^-)$, 1404 $\nu_s(COO^-)$, 1364 $\nu_s(COO^-)$.

X-ray diffraction analysis. Single-crystal X-ray diffraction data for **I** and **II** were collected on a computer-controlled Bruker APEX-II CCD diffractometer equipped with graphite-monochromated MoK_α radiation with radiation wavelength 0.71073 Å by using ω–φ scan mode at room temperature. Semiempirical multiscan absorption corrections were applied using SADABS [18] and the program SAINT [19] was used for integration of the diffraction profiles. Both structures were solved by direct methods and refined with the full-matrix least-squares technique using the SHELXS-97 and SHELXL-97 programs [20]. Anisotropic thermal parameters were assigned to all non-hydrogen atoms. The organic hydrogen atoms were generated geometrically. Details for crystallographic data were listed in Table 1, and selected bond lengths and angles were given in Table 2. Hydrogen-bonding parameters for **I** and **II** were shown in Table 3. Supplementary material has been deposited with the Cambridge Crystallographic Data Centre (nos. 664900 (**I**) and 664899 (**II**); deposit@ccdc.cam.ac.uk or http://www.ccdc.cam.ac.uk).

RESULTS AND DISCUSSION

Phase-pure crystals of **I** and **II** were successfully prepared under similar hydrothermal conditions in basic medium. Obviously, the introduction of aqueous NaOH solution is to make HNA ligand deprotonation and facilitate its coordination with Pb^{2+} ion. Additionally, complexes **I** and **II** are air stable, insoluble in common organic solvents and can retain their crystalline integrity at ambient conditions for a considerable length of time.

In the IR spectra, the weak absorption peaks appeared at 3051 cm^{-1} (for both **I** and **II**) could be ascribed to the C–H stretching vibrations of aromatic ring. An absence of a characteristic band at 1675 cm^{-1} in **I** and **II** indicates the complete deprotonation of HNA ligand by NaOH [21], which is consistent with the results of single crystal structure determinations. In addition, I shows characteristic peaks at 1594, 1545, and 1470, 1430, 1356 cm^{-1} for asymmetric (ν_{as}) and symmetric (ν_s) stretching vibrations of carboxylate group. For **II**, the asymmetric and symmetric stretching vibrations for carboxylate group appear at 1598, 1541, and 1456, 1404, 1364 cm^{-1}. The different splits

Table 1. Crystallographic data and structure refinement summary for **I** and **II**

Parameter	Value	
	I	**II**
Formula weight	705.71	627.61
Crystal size, mm	0.24 × 0.22 × 0.18	0.28 × 0.12 × 0.10
Crystal system	Triclinic	Monoclinic
Space group	$P\bar{1}$	$P2_1/c$
a, Å	8.7078(15)	13.6990(7)
b, Å	11.294(2)	21.8430(11)
c, Å	14.633(3)	7.6150(4)
α, deg	70.255(2)	90
β, deg	77.317(2)	98.3630(10)
γ, deg	81.879(2)	90
V, Å^3	1317.9(4)	2254.4(2)
Z	2	4
ρ_{calcd}, g/cm^3	1.778	1.849
μ_{Mo}, mm^{-1}	6.442	7.518
F(000)	684	1204
θ Range, deg	2.40–25.01	1.77–25.01
Range of reflection indices	$-9 \leqslant h \leqslant 10$, $-12 \leqslant k \leqslant 13$, $-14 \leqslant l \leqslant 17$	$-16 \leqslant h \leqslant 15$, $-25 \leqslant k \leqslant 21$, $-8 \leqslant l \leqslant 9$
Reflections collected/unique	6993/4544	12208/3977
R_{int}	0.0267	0.0212
Parameters	352	298
GOOF on F^2	1.031	1.043
R ($I > 2\sigma(I)$)*	$R_1 = 0.0368$, $wR_2 = 0.0865$	$R_1 = 0.0192$, $wR_2 = 0.0418$
R (all reflections)*	0.0503/0.0907	0.0253/0.0433
$\Delta\rho_{max}/\Delta\rho_{min}$, e Å^{-3}	1.003/–1.135	0.605/–0.683

* $R_1 = \Sigma(||F_o| - |F_c||)/\Sigma|F_o|$, $wR_2 = [\Sigma w(|F_o|^2 - |F_c|^2)^2/\Sigma w(F_o^2)]^{1/2}$.

Table 2. Selected bond lengths (Å) and angles (deg) for **I** and **II**

Bond	d, Å	Bond	d, Å
	I		
Pb(1)–N(1)	2.549(6)	Pb(1)–N(2)	2.668(5)
Pb(1)–O(1)	2.737(6)	Pb(1)–O(2)	2.518(5)
Pb(1)–O(4)	2.297(5)		
	II		
Pb(1)–O(1)	2.662(2)	Pb(1)–O(2)	2.326(2)
Pb(1)–N(1)	2.520(3)	Pb(1)–O(3)	2.296(2)
Angle	ω, deg	Angle	ω, deg
	I		
O(4)Pb(1)O(2)	81.88(17)	O(4)Pb(1)N(1)	72.21(18)
O(2)Pb(1)N(1)	84.03(18)	O(4)Pb(1)N(2)	84.97(17)
O(2)Pb(1)N(2)	146.13(18)	N(1)Pb(1)N(2)	62.22(16)
O(4)Pb(1)O(1)	77.1(2)	O(2)Pb(1)O(1)	49.65(19)
N(1)Pb(1)O(1)	127.3(2)	N(2)Pb(1)O(1)	153.91(19)
	II		
O(2)Pb(1)O(1)	51.07(8)	O(3)Pb(1)O(1)	101.57(10)
N(1)Pb(1)O(1)	128.43(8)	O(3)Pb(1)N(1)	77.85(9)
O(2)Pb(1)N(1)	78.05(9)	O(3)Pb(1)O(2)	83.91(9)

Table 3. Hydrogen bond lengths (Å) and bond angles (deg) for **I** and **II***

Contact D–H···A	Distance, Å			Angle D–H···A, deg
	D–H	H···A	D···A	
		I		
C(3)–H(3)···O(3)^{i}	0.93	2.54	3.412(4)	156
C(5)–H(5)···O(4)^{ii}	0.93	2.59	3.439(3)	152
		II		
C(3)–H(3)···O(4)^{i}	0.93	2.55	3.381(1)	149
C(14)–H(14)···O(1)^{ii}	0.93	2.53	3.263(2)	136

* Symmetry codes: ^{i} $1 + x, y, z$; ^{ii} $1 - x, -y, 1 - z$ (**I**); ^{i} $x, 1/2 - y, -1/2 + z$; ^{ii} $x, 1/2 - y, 1/2 + z$ (**II**).

and separations between ν_{as} and ν_{s} indicates the coexistence of the multiple coordination modes [22]. Thus, the results of IR spectra are well agreement with those of crystal structure determinations.

As shown in Fig. 1a, the asymmetric unit of I consists of one crystallographically independent Pb^{2+} ion, one neutral 2,2'-Bipy ligand and a pair of unique NA^{-} anion in different binding modes. The sole unique Pb^{2+} ion in **I** is five-coordinated in a distorted tetragonal pyramidal coordination geometry defined by two N atoms from one chelating 2,2'-Bipy ligand and three carboxylate O donors from two individual NA^{-} anions. The equatorial plane of tetragonal pyramidal is defined by two carboxylate O (O(1) and O(2)) and two pyridyl N donors (N(1) and N(2)), and the axial position is occupied by one carboxylate O donor (O(4)) from another NA^{-} anion. The bond length of the axial Pb–O is 0.44 and 0.22 Å shorter than those in the equatorial plane (Table 2). The $Pb–O_{carboxylate}$ and Pb–N distances are in the region of 2.297 to 2.737 Å (Table 2), falling into the normal range of Pb(II)-based complexes with mixed carboxylao and/or pyridyl ligands [23]. The active lone pair of electrons of Pb^{2+} is thought to be located in the vacancy of coordination environment, resulting a shortening of Pb-donor bond lying in the opposite side of the metal center [12]. Due to the bond distance of Pb–O(4) is shortest in all the coordinated bonds, the 6*s* lone pair of electrons of Pb^{2+} can be speculated to lie in the opposite direction of Pb–O(4) bond.

Acting as a typically bidentate chelating ligand, neutral 2,2'-Bipy molecule binds Pb^{2+} ion in an asymmetric bidentate mode with the Pb–N(2) bond distance 0.12 Å longer than that of Pb–N(1) (Table 2). By contrast, the two unique NA^{-} ligands in **I** adopt two different binding modes. One presents its carboxylate group to Pb^{2+} ion in a bidentate chelating coordination mode, and the second carboxylate group belonging to the other NA^{-} ligand exhibit a monodentate fashion to complete the coordination sphere of the central Pb^{2+} ion.

Each mononuclear molecules of **I** are joined together to form a 1D chain through intermolecular C–H···O weak hydrogen bonding interactions (Fig. 1b). The distances of H and C atoms to the acceptor O atom from carboxylate moiety of adjacent NA^{-} anion are 2.54 and 3.41 Å, respectively, and the involved angle (angle CHO) is 156° (Table 3). Furthermore, the adjacent 1D chains are further linked together to form 2D supramolecular layer through π···π stacking interactions and the interchain C–H···O hydrogen bonding (Fig. 1c). The π···π stacking interaction are produced between phenyl ring of NA^{-} anions and bipyridyl rings of 2,2'-Bipy ligands with the centroid-centroid distance of ca. 3.507 Å and a dihedral angle of ca. 2.271°. For the molecular hydrogen bonding interactions, the distances of H and C atoms to the acceptor O atom from carboxylate moiety of adjacent NA^{-} anion are 2.59 and 3.44 Å, respectively, and the involved angle (angle CHO) is 152° (Table 3).

Different from **I**, complex **II** exhibits a centrosymmetric binuclear structure bridged by 4,4'-Bipy ligand. As shown in Fig. 2a, the asymmetric unit of **II** contains one crystallographically independent Pb(II) site, two NA^{-} anions in different binding modes, and a half of 4,4'-Bipy ligand. The unique Pb^{2+} ion is four-coordinated by three O atoms from two NA^{-} anions and one N atom from 4,4'-Bipy ligand, forming a distorted PbO_3N tetrahedral geometry. All the bond distances and angles around Pb^{2+} ion fall into the normal range (Table 2) [23]. Similar to **I**, the 6*s* lone pair of electrons of Pb^{2+} in **II** can be speculated to lie in the opposite direction of shortest Pb–O(3) bond, resulting a vacancy of coordination environment of metal center [12].

Although NA^{-} anions in **II** exhibit the same of binding mode as those in **I**, bidentate chelating and monodentate coordination mode, the separations of Pb and O atoms are slightly shorter than the contrasts in **I** correspondingly, which may due to the different

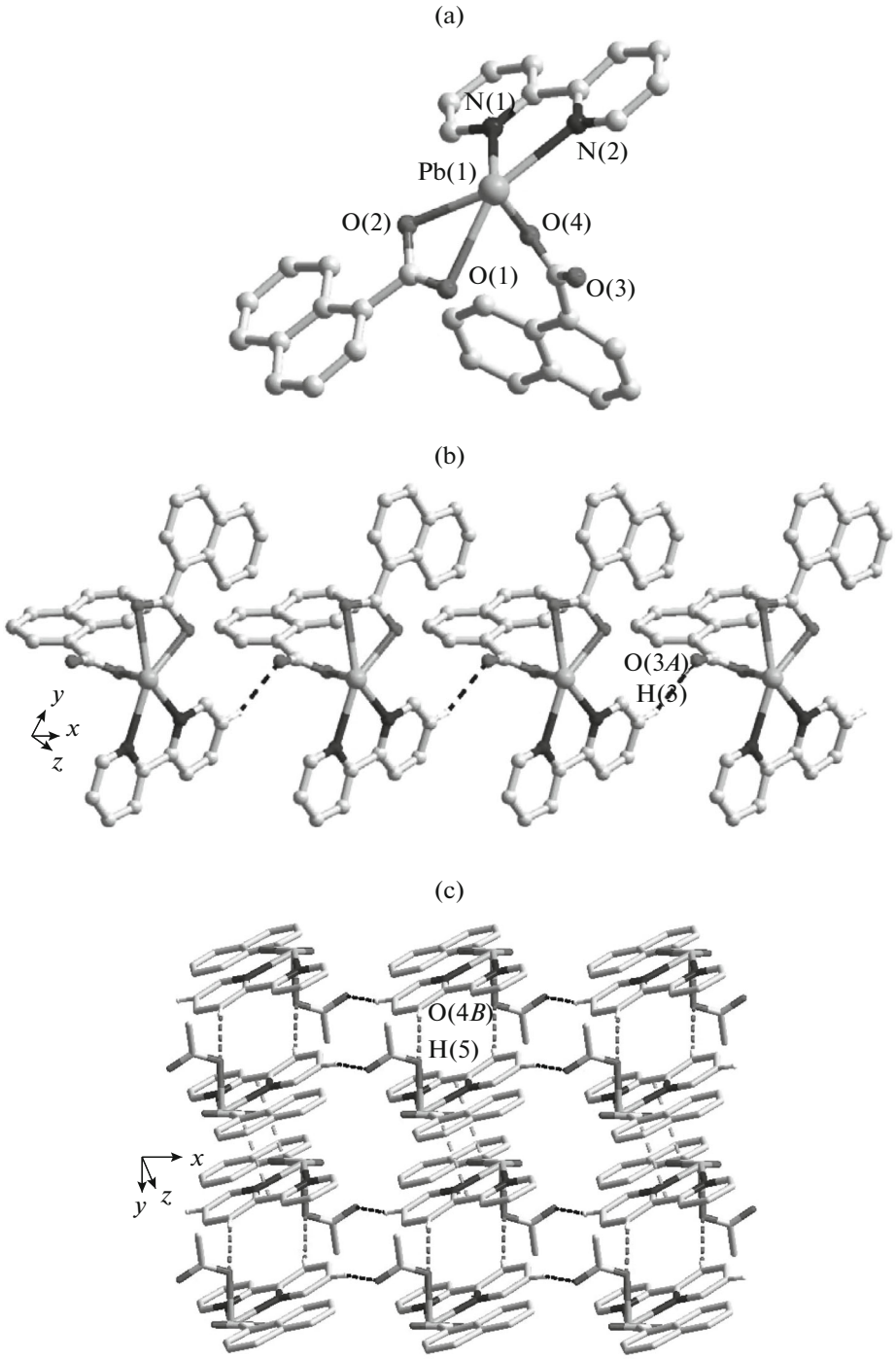

Fig. 1. Mononuclear structure of **I** (a) (hydrogen atoms were omitted for clarity); 1D chain of **I** connected by intermolecular C(3)–H(3)···O(3) hydrogen bonds interactions (b) (only H atoms involved in hydrogen bonds were included); 2D supramolecular layer of **I** formed by π···π stacking interactions and intermolecular C(5)–H(5)···O(4) hydrogen bonding (c) (the naphthalene group of monodentate NA^- ligand were omitted for clarity, only H atoms involved in hydrogen bonds were included).

geometry of the metal centers. Furthermore, the 4,4'-Bipy ligand adopt bidentate bridging coordination mode and connect two adjacent Pb^{2+} ions together to form a binuclear motif with adjacent Pb···Pb distance of ca. 12.1088 Å. Moreover, the separation between the central Pb^{2+} ion and the N atom is slightly shorter than that in **I**, which may be ascribed to the different coordination mode of N-containing ligands bearing different aromatic skeletons (Table 2).

As shown in Fig. 2b, the adjacent discrete binuclear $[Pb_2(NA)_4(4,4'\text{-Bipy})]$ molecules are arranged into a 1D chain by the weak intermolecular π···π stacking

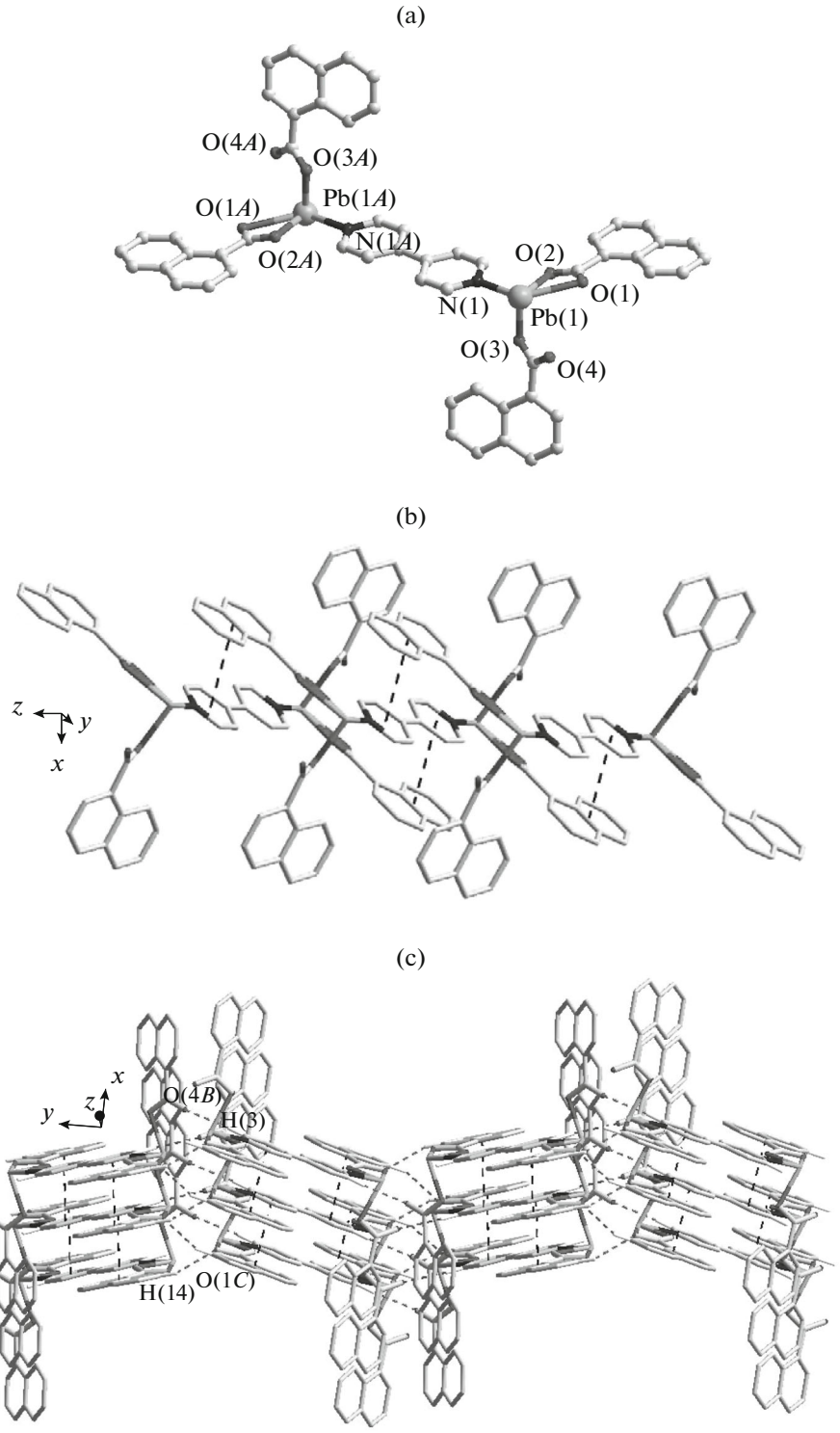

Fig. 2. Binuclear entity of **II** (a) (hydrogen atoms were omitted for clarity. Symmetry codes: $A = 1 - x, 1 - y, -z$); 1D double chain of **II** extended by intermolecular π···π stacking interactions (b) (hydrogen atoms were omitted for clarity); quasi-2D network of **II** formed by intermolecular C(3)–H(3)···O(4) and C(14)–H(14)···O(1) hydrogen bonds (c) (only H atoms involved in hydrogen bonds were included).

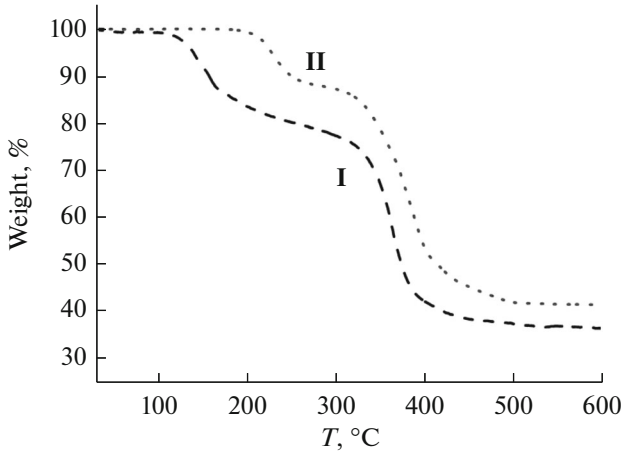

Fig. 3. TG curves for **I** and **II**.

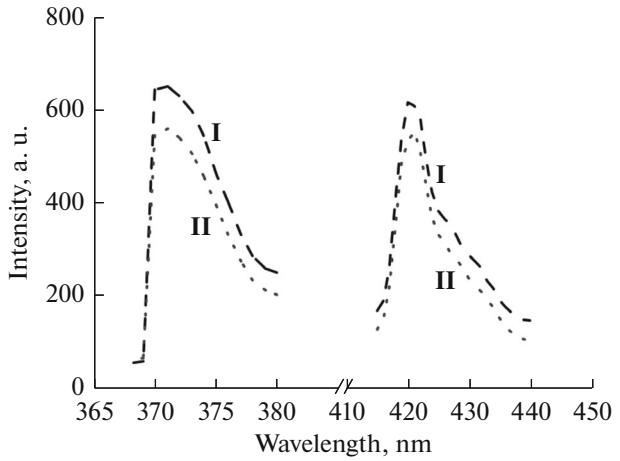

Fig. 4. Solid-state emissions of **I** and **II** at room temperature.

interactions between the naphthalene rings of the NA^- anions and the pyridyl rings from 4,4'-Bipy ligands with the centroid-centroid separation of ca. 3.756 Å and dihedral angle of ca. 3.279°. The quasi-2D network of **II** is formed by two-fold intermolecular C–H···O weak hydrogen bonding interaction (Fig. 2c). The separations between C (donor) and O (acceptor) and C–H···O angle is 3.38 Å, 149° and 3.26 Å, 136°, respectively.

Apparently, the NA^- anion in **I** and **II** exhibit the same binding modes (bidentate chelating and monodentate coordination mode), and the bipyridyl co-ligand govern the dissociation or dimerization of the mononuclear structure through the bidentate chelating or bridging modes as well as the binding numbers of the Pb^{2+} ion.

To explore their thermal stability, TGA experiments of **I** and **II** were carried out and the results were presented in Fig. 3. As a result, I can be thermally stable up to 110°C and is followed by a continuous two-step weight-loss stage between 110 and 476°C. The obvious weight-loss stage is corresponding to the broken of the mononuclear motif and the decomposition of the mixed ligands. The remained substance beyond 476°C is calculated to be PbO (obsd. 33.2%, calcd. 31.6%). The release of 4,4'-Bipy ligand in **II** is ranged from 185 to 260°C (obsd. 12.3%, calcd. 12.4%), the remaining compound does not lose its weight until 310°C. The secondly weight-loss stage between 310 and 497°C is ascribed to the loss of NA^- anions (obsd. 48.8%, calcd. 52.0%). The remaining PbO fragment is stable upon further heating until it ends at 800°C.

Constructed from bulky π-conjugated NA^- and bipyridine ligands, complexes **I** and **II** can be hopefully applied as luminescent materials. Thus, the solid-state emission spectra at room temperature are examined and the results are depicted in Fig. 4. Upon excitation at 372 nm, both complexes display blue photoluminescence with maximum emission at 422 nm. It is documented that isolated HNA species give a broad fluorescent emission at 420 nm under comparable conditions [15], so the analogous emission band of **I** and **II** can be assigned to the intraligand charge transfer of NA^- anions. The slight red shift of the emission wavelength is probably resulting from the energy gap between the intraligand molecular orbitals decrease because of the deprotonation of HNA and the coordination behavior of NA^- to Pb^{2+} ion [14].

In summary, two novel Pb(II)-naphtholate complexes possessing discrete mononuclear and binuclear structure modulated by bipyridyl co-ligands have been hydrothermally synthesized and structurally characterized. Structural analysis reveals that the NA^- anions is significantly dominate the formation of the limited-nuclear motifs and the bipyridyl co-ligands play key roles with the dissociation/dimerization of the monoculear units as well as the coordiantional numbers of the metal centers. The 6*s* lone pair of electrons of Pb^{2+} in both complexes has a stereochemistry activity resulting the distribution of the Pb–O and Pb–N bonds in a hemisphere. Ascribing into the NA^--based intraligand charge transfer, both the two complexes exhibit strong fluorescent emissions, suggest their potential applications as luminescent materials.

ACKNOWLEDGMENTS

This present work was supported by the Science Foundation of Shaanxi University of Technology (SLGQD13-4), which is gratefully acknowledged.

REFERENCES

1. Li, D.S., Zhang, P., Zhao, J., et al., *Cryst. Growth Des.*, 2012, vol. 12, no. 4, p. 1697.
2. Wang, X.L., Chen, Y.Q., Gao, Q., et al., *Cryst. Growth Des.*, 2010, vol. 10, no. 5, p. 2174.

3. Song, F.J., Wang, C., Falkowski, J.M., et al., *J. Am. Chem. Soc.*, 2010, vol. 132, no. 43, p. 15390.
4. Song, F.J. Wang, C., and Lin, W.B., *Chem. Commun.*, 2011, vol. 47, p. 8256.
5. Du, L.T., Lu, Z.Y., Zheng, K.Y., et al., *J. Am. Chem. Soc.*, 2013, vol. 135, no. 2, p. 562.
6. Tzeng, B.C., Chang, T.Y., Wei, S.L., et al., *Chem. Eur. J.*, 2012, vol. 18, no. 16, p. 5105.
7. Liang, L., Peng, G., Ma, L., et al., *Cryst. Growth Des.*, 2012, vol. 12, no. 3, p. 1151.
8. Shimoni-Livny, L., Glusker, J.P., and Bock, C.W., *Inorg. Chem.*, 1998, vol. 37, no. 8, p. 1853.
9. Zhang, Y., Wang, J., Yan, X.F., et al., *Microporous Mesoporous Mater.*, 2014, vol. 184, p. 15.
10. Zhang, K.L., Chang, Y., Hou, C.T., et al., *CrystEngComm*, 2010, vol. 12, p. 1194.
11. Yang, J., Ma, J.F., Liu, Y.Y., et al., *Cryst. Growth Des.*, 2009, vol. 9, no. 4, p. 1894.
12. Hu, M.L., Morsali, A., and Aboutorabi, L., *Coord. Chem. Rev.*, 2011, vol. 255, nos. 23–24, p. 2821.
13. Kole, G.K., Peedikakkal, A.M.P., Toh, B.M.F., et al., *Chem. Eur. J.*, 2013, vol. 19, no. 12, p. 3962.
14. Yang, E.C., Dai, P.X., Wang, X.G., et al., *Transition Met. Chem.*, 2007, vol. 32, no. 2, p. 228.
15. Yang, E.C., Dai, P.X., Wang, X.G., et al., *Z. Anorg. Allg. Chem.*, 2009, vol. 635, no. 2, p. 346.
16. Hou, Z.J., Wang, X.G., Dai, P.X., et al., *Chin. J. Struct. Chem.*, 2012, vol. 31, no. 9, p. 1295.
17. Dai, P.X., Yang, E.C., and Zhao, X.J., *Russ. J. Coord. Chem.*, 2015, vol. 41, no. 1, p. 16.
18. Sheldrick, G.M., *SADABS, Program for Empirical Absorption Correction of Area Detector Data*, Göttingen: Univ. of Göttingen, 1996.
19. *SAINT, Software Reference Manual*, Madison: Bruker AXS, 1998.
20. Sheldrick, G.M., *SHELXTL, Structure Determination Software Programs*, Madison: Bruker Analytical X-ray System, Inc., 2001.
21. Bellamy, L.J., *The Infra-Red Spectra of Complex Molecules*, New York: Wiley, 1958.
22. Cao, R., Shi, Q., Sun, D.F., et al., *Inorg. Chem.*, 2002, vol. 41, no. 23, p. 6161.
23. Deng, D.S., Liu, L.L., Ji, B.M., et al., *Cryst. Growth Des.*, 2012, vol. 12, no. 11, p. 5338.